

Synthesis and Biological Activity of Phosphonate Analogues and Geometric Isomers of the Highly Potent Phosphoantigen (*E*)-1-Hydroxy-2-methylbut-2-enyl 4-Diphosphate

Angélique Boëdec,[†] Hélène Sicard,[†] Jean Dessolin,^{||} Gaëtan Herbet,[§] Sophie Ingoure,[†] Cédric Raymond,[†] Christian Belmant,[†] and Jean-Louis Kraus^{*‡}

Innate Pharma, 121 Ancien Chemin de Cassis, 13009 Marseille, France, UMR 5248 CBMN, CNRS-Université Bordeaux I-ENITAB, Institut Européen de Chimie et Biologie (IECB), 2 rue Robert Escarpit, 33607 Pessac Cedex, France, Spectropole, Université Paul Cézanne, Avenue Escadrille Normandie Niémen, 13397 Marseille Cedex 20, France, and Laboratoire de Chimie Biomoléculaire, IBDML, UMR 6216, CNRS, Université de la Méditerranée, Parc scientifique de Luminy, 13288 Marseille cedex 09, France

Received September 5, 2007

$\gamma\delta$ -T-lymphocytes contribute to innate immunity and are selectively activated by nonpeptide phosphorylated molecules (so-called phosphoantigens) produced by organisms responsible for causing a broad range of infectious diseases. $\gamma\delta$ -T-cells are also activated by synthetic phosphoantigens and are cytotoxic to tumor cells. Here we report the synthesis, NMR characterization, and comparative biological evaluation of new pyrophosphate, phosphonate, and pyrophosphonate monoesters whose structures correspond to isosteric analogues and stereoisomers of the highly potent isoprenoid metabolite (*E*)-1-hydroxy-2-methylbut-2-enyl 4-diphosphate called HDMAPP (hydroxy-dimethyl-allyl pyrophosphate). Both pyrophosphate and pyrophosphonate series elicit promising $\gamma\delta$ -T-cell stimulatory responses in vitro, the pyrophosphonate ester (C-HDMAPP) being by far more stable than its parent pyrophosphate ester (HDMAPP) with improved ADMET properties and a similar pharmacodynamic profile based on in vivo studies in nonhuman primate. In both series, we found that *E*-stereoisomers are the most active derivatives and that *Z*-stereoisomers show very marginal bioactivity levels. These results indicate that the use of bioisosteric analogues of HDMAPP may represent promising new leads for immunotherapy.

Introduction

Numerous natural and non-natural bacterial phosphoantigens have been described in the literature. Their use to stimulate $\gamma\delta$ -T-cells of the immune system as well as the structure of the human $\gamma\delta$ -T-cell antigen receptor have been reported.^{1–3} Isopentenyl pyrophosphate (IPP,^a **1**) was the first structurally identified natural ligand for human $\gamma\delta$ -T-lymphocytes,⁴ and based on this structure, the synthetic phosphoantigen bromohydrin of isopentyl pyrophosphate⁵ (**2**) known as BrHPP was developed and is now in Phase II clinical trials in oncology and infectious disease (metastatic renal cell carcinoma, follicular lymphoma, chronic myeloid leukemia, metastatic melanoma and chronic hepatitis C). More recently, (*E*)-1-hydroxy-2-methylbut-2-enyl 4-diphosphate (HDMAPP, **3**), an intermediate of isoprenoid biosynthesis in the deoxyxylulose phosphate pathway,^{6–8} was identified and was found to be recognized very selectively by $\gamma\delta$ -T-cells and is so far the most potent phosphoantigen described. Therefore, the selection of compounds for this study was guided by the aforementioned three structures (Figure 1).

Despite the report of several pyrophosphate analogues of potential clinical importance, the possibility exists to improve their ADMET (absorption distribution metabolism excretion and toxicity) properties, mainly bioavailability, by using medicinal chemistry concepts to design new analogues. Based on the well-

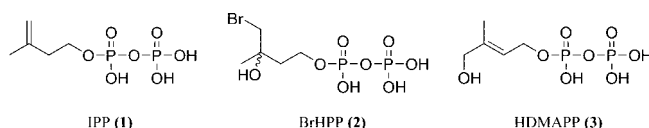


Figure 1. Structure of active known phosphoantigens.

known bioisosteric concept,^{9,10} we report herein the synthesis and the $\gamma\delta$ -T-cell activating properties of new phosphonate (**7E**, **7Z**, **8**) and pyrophosphonate bioisosters (**5E**, **5Z**, **6**), as well as the synthesis of new pyrophosphate analogues (**4E** and **4Z**) bearing different substituted butenyl chains that have never been reported (Figure 2). Because the phosphonate moieties are much less susceptible to chemical or enzymatic hydrolysis than their corresponding phosphate counterparts, it was expected that these new phosphonate and pyrophosphonate analogues could have improved pharmacological properties, mainly better stability in biological media. To assess the $\gamma\delta$ -T-cell stimulatory properties of the new phosphonate analogues, pyrophosphate isomers (**3E** and **3Z**) are included in this study for comparative purposes, their synthesis having already been described.^{6,7}

T-lymphocytes that express the V γ 9V δ 2 ($\gamma\delta$) receptor and represent 1 to 5% of total blood lymphocytes in a healthy individual have function equivalent only in nonhuman primate (NHP) species. Old world macaques, such as *M. fascicularis*, the cynomolgus monkey, are one of the classical species used to evaluate the safety of immuno-modulating drugs in development. We have recently reported the complete pharmacological (dosing and scheme of administration, phenotypical, and functional analyses of target cells), pharmacokinetics, and safety profiles of **2** in cynomolgus.¹¹ Currently, second-generation $\gamma\delta$ -agonist candidates for pharmaceutical development are undergoing preclinical selection steps, including steps aimed at comparing their activity in vitro in standardized bioassays, their potential metabolic and excretion properties, and ultimately, their

* To whom correspondence should be addressed. Tel.: 33 (0)491829141. Fax: 33 (0)491829416. E-mail: kraus@luminy.univ-mrs.fr.

[†] Innate Pharma.

^{||} UMR 5248 CBMN.

[§] Spectropole, Université Paul Cézanne.

[‡] IBDML, UMR 6216, CNRS.

^a Abbreviations: IPP, isopentenyl pyrophosphate; BrHPP, bromohydrin pyrophosphate; HDMAPP, hydroxy-dimethyl-allyl pyrophosphate; ADMET, absorption distribution metabolism excretion and toxicity; NHP, nonhuman primate; HPAEC, high performance anion exchange chromatography.

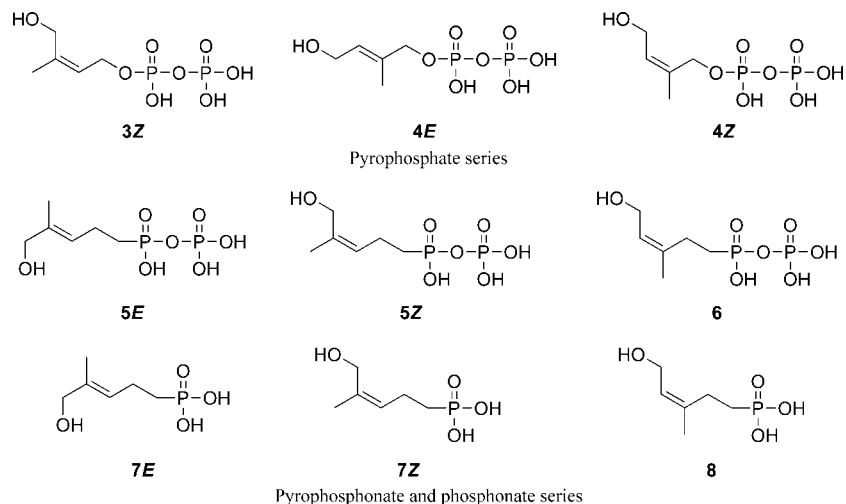
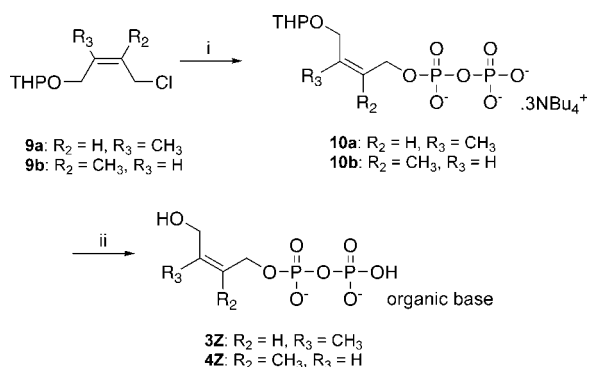


Figure 2. Structures of the pyrophosphate, pyrophosphonate, and phosphonate analogues.

Scheme 1^a



^a Reagents and conditions: (i) (Bu₄N)₃HP₂O₇, CH₃CN, 0 °C to rt; (ii) Dowex 50WX8 H⁺ form, crystallization with an organic base.

activity and safety profiles in the primate. We report here results arising from such studies of certain of the $\gamma\delta$ -agonists.

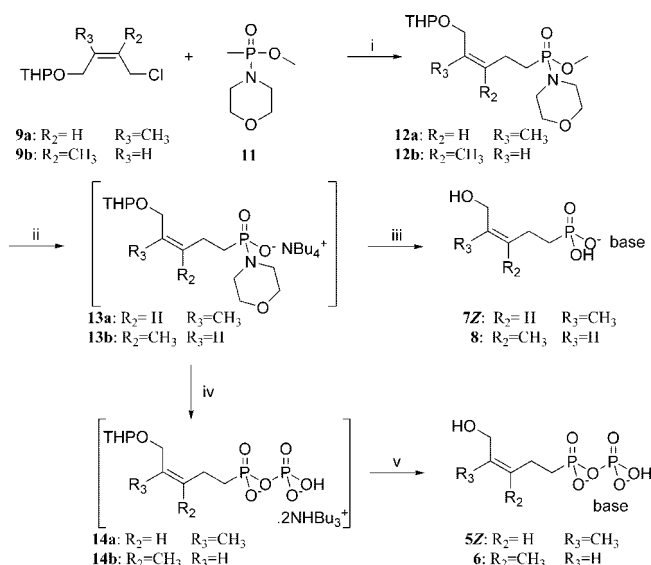
Results and Discussion

Chemistry. Key compound (*Z*)-4-chloro-2-methyl-1-(tetrahydropyran-2-yloxy)but-2-en (**9a**) and its isomer (*Z*)-1-chloro-2-methyl-4-(tetrahydropyran-2-yloxy)but-2-en (**9b**) have been obtained as described in the literature.^{12,13} Intermediates **9a** and **9b** (1 equiv) were reacted with 1.5 equiv of (Bu₄N)₃HP₂O₇ in acetonitrile at room temperature, the corresponding salt **3Z** and **4Z** were, respectively, recovered with 35 and 51% yield after standard ion-exchange purification and crystallization (Scheme 1).

Analogues **5Z** and **7Z** on the one hand and analogues **8** and **6** on the other hand were obtained from the corresponding precursors **9a** and **9b** using the synthetic sequence described in Scheme 2. The phosphorylating agent **11** could be readily prepared by an already described two-step procedure.¹⁴ Treatment of commercially available methylphosphonic dichloride with morpholine followed by the addition of methanol and triethylamine gave, after distillation, homogeneous **11** in 77% yield.

NMR Studies. One of the major issues of this work was to study the influence of the geometry of *Z* and *E* of both pyrophosphonate and pyrophosphate derivatives on $\gamma\delta$ -T-cell stimulatory properties. For this purpose, the *Z*- and *E*-conformation of the new synthesized analogues have been unambiguously

Scheme 2^a

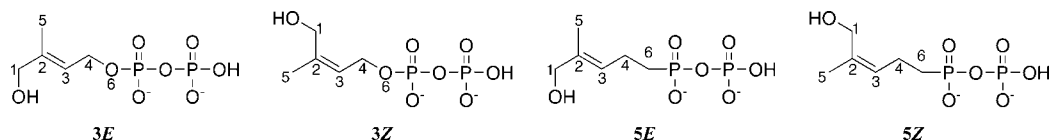


^a Reagents and conditions: (i) BuLi, THF, -78 °C, **12a** and **12b** 34% each; (ii) TBAOH 0.8 M in MeOH, reflux, 2 days; (iii) Dowex 50WX8 H⁺ form, crystallization with an organic base, **7Z** (13%) and **8** (20%); (iv) H₃PO₄, TBA, pyridine; (v) *i*-PrOH/NH₄OH, Dowex 50WX8 H⁺ form, crystallization with an organic base, **5Z** (23%) and **6** (44%).

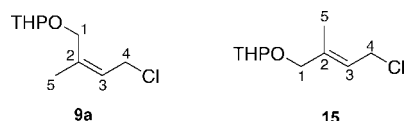
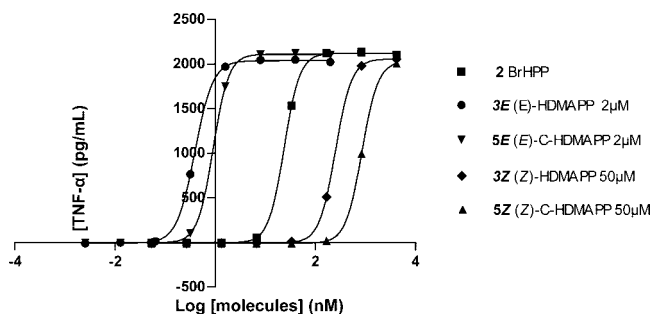
assigned (Figure 3) based on NMR studies. Specific chemical shift assignments are shown in Table 1.

The geometries of compounds **3E/3Z** and **5E/5Z** were thus established on the basis of ¹³C NMR studies. Gamma effects were observed on both C-1 and C-5 carbons. A highfield C-1 effect was observed between *E*-isomers and their corresponding *Z*-isomers (respectively, $\Delta\delta$ **3E/3Z** = 6.6 ppm and $\Delta\delta$ **5E/5Z** = 7.6 ppm), and a low field C-5 effect was observed between both isomers (respectively, $\Delta\delta$ **3E/3Z** = 7.4 ppm and $\Delta\delta$ **5E/5Z** = 7.5 ppm). This confirmed the assigned geometries for both *Z* and *E* geometries of analogues **3** and **5**.

NOESY experiments (data not shown) on *Z*-isomer **9a** and its corresponding *E*-isomer **15** (already described by Amslinger et al.)⁶ showed a strong NOE effect between protons H3/H5 for **9a** compared to its corresponding *E*-analogue **15**. Specific gamma effects were also observed for both isomers; the shifts for carbons C-1 and C-5 (Figure 4) were, respectively, $\Delta\delta$ 6.5 ppm and $\Delta\delta$ 5.6 ppm, confirming the assigned geometries.

**Figure 3.** Structures of **3E**, **3Z**, **5E**, and **5Z**.**Table 1.** ^{13}C NMR Spectral Data for Compounds **3E**, **3Z**, **5E**, and **5Z**^a

	3E		3Z	$\Delta\delta$ (ppm)	5E		5Z	$\Delta\delta$ (ppm)
1	66.7	γ	60.1	6.6	67.8	γ	60.2	7.6
2	140.2		140.0		134.9		134.2	
3	120.5 d (7.5)		123.5 d (8.0)		126.8 d (17.4)		128.8 d (17.6)	
4	62.8 d (4.6)		62.2 d (4.4)		21.5 d (4.8)		21.5 d (3.8)	
5	13.4	γ	20.8	7.4	13.3	γ	20.8	7.5
6					27.9 d (137.5)		28.3 d (137.0)	

^a J in hertz.**Figure 4.** Structures of *E* and *Z* key compounds.**Figure 5.** In vitro titration of $\text{V}\gamma 9\text{V}\delta 2$ T-cell-stimulating bioactivity by phosphoantigens **3** and **5** compared to **2**.

Complementary to the NMR characterization, the purity assessment of the different compounds was established by ion chromatography using suppressed conductivity detection.^{15,16}

Biological Activity. Comparative In Vitro Evaluation of Phosphoantigens Using TNF- α Release Assay. First we investigated the ability of analogues (**3E**, **3Z**, **4E**, **4Z**, **5E**, **5Z**, **6**, **7E**, **7Z**, **8**) to stimulate responder cells, primary polyclonal human $\text{V}\gamma 9\text{V}\delta 2$ T-cells (rate >90% in flow cytometry), expanded in vitro by BrHPP/IL2 stimulation. These responder cells are used to test the analogues by measurement of TNF- α release in a standardized assay. The responsive cells are restimulated with ascending concentrations of the new synthesized analogues. It was observed that the release of TNF- α by the cells, determined through an ELISA dosage, is a function of the phosphoantigen concentration. EC_{50} values represent the required phosphoantigen concentration to reach 50% of the optimal response (phosphoantigen concentration inducing maximal activity). Graphical comparison for the isomers **3E**, **3Z**, **5E**, and **5Z** compared to **2** are represented in Figure 5.

Biological activities of the different phosphoantigens are summarized in Table 2. The stimulatory activities of already known $\gamma\delta$ -agonists are given as ref 1 and 2.

Comparative In Vivo Evaluation of **3E versus **5E** in Nonhuman Primate Model.** Groups of 3–5 cynomolgus received increasing doses of **3E** i.v., ranging from 0.02 to 2.5 mg/kg. Other groups of 2–4 animals received **5E**, from 0.02 to 10 mg/kg (the difference in doses tested only reflecting the

respective amounts of each compound available at that time). All animals were cotreated with daily s.c. low doses IL-2 to sustain $\gamma\delta$ -T-cell proliferation.¹¹ $\gamma\delta$ -Kinetics of amplification is comparable between **5E** and **3E** and very close to what was observed initially with BrHPP,¹¹ with a peak around days 5–6 and back to basal at days 11–15 (Figure 6). Thus, it can be considered that any phosphoantigen evaluated so far in vivo has the same qualitative effect on $\gamma\delta$ -cells. For both **3E** and **5E**, the lowest dose tested (0.02 mg/kg) provides a significant increase in $\gamma\delta$ -cells. At 5 and 10 mg/kg, **5E** seems to have reached its maximal effect. For both molecules, 2.5 mg/kg induces between 40 and 60% of circulating $\gamma\delta$ -cells, which can be considered equivalent due to high and well-known interindividual heterogeneity. When expressed as fold-increase in blood $\gamma\delta$ -cells as compared to predose, expansion induced by **3E** seems somewhat higher than that by **5E**, but this difference is not statistically significant. We also found (data not shown) in comparative excretion after i.v. administration to rats of the radiolabeled isotopes of **3E** and **5E** that **5E** was totally excreted; in contrast, only 80% of **3E** was recovered after 7 days and that 50% of **3E** versus 80% of **5E** was excreted in urine.

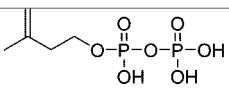
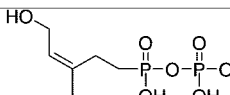
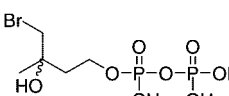
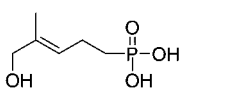
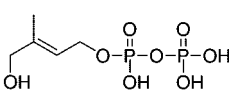
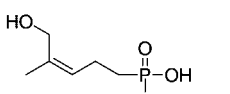
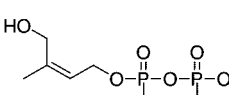
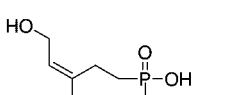
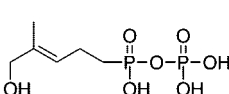
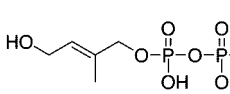
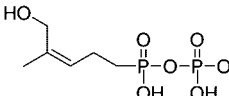
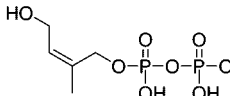
Comparative Chemical Stabilities of **3E and **5E**.** One of the main reasons to synthesize the new phosphonate and pyrophosphonate was their possible enhanced stability compared to their corresponding phosphate and pyrophosphate analogues. Indeed, data already published about pyrophosphate **2** show that its half-life in vivo was quite short, probably not exceeding a few minutes.¹¹ To test whether pyrophosphonate have enhanced stability compared to pyrophosphate analogues, we have subjected aqueous solutions of pyrophosphate **3E** and pyrophosphonate **5E** to various conditions of temperature, pH, and stress. The results obtained are summarized in Table 3.

As expected, the pyrophosphonate derivative **5E** is far more stable than pyrophosphate **3E**, regardless of the conditions of temperature, acidic media, or oxidizing condition (H_2O_2).

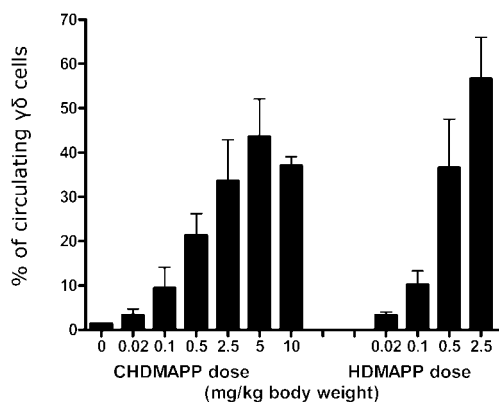
Discussion

Among the new synthesized derivatives, compound **3E** appears to be the most active derivative ($\text{EC}_{50} = 0.39$ nM); it is at least 600 times more potent than its corresponding *Z*-analogue (**3Z**, $\text{EC}_{50} = 252$ nM). This result clearly shows that the *E*-isomer is the preferred geometry for optimal $\gamma\delta$ -T-cell stimulatory activity, compared to its corresponding *Z*-isomer. The same results were observed for the compound **4E** ($\text{EC}_{50} = 93.5$ nM) compared to **4Z** ($\text{EC}_{50} > 100000$ nM) and its pyrophosphonate analogue **6** ($\text{EC}_{50} > 100000$ nM), which were emphasized by the result of the monophosphate **7E** versus **7Z**.

Table 2. Results of $\gamma\delta$ -T-Cell Stimulation by New (*Z*- and *E*-)Hydroxy-methyl-butenyl Pyrophosphonate and Pyrophosphate Isomers

Compound	EC ₅₀ (nM)	Compound	EC ₅₀ (nM)
	81076		>100,000
	23.85		2530
	0.39		78731
	252.2 ^a		>100,000
	0.91		93.5
	852 ^b		>100,000

^a Pyrophosphate **3Z** contains 2% (HPAEC relative area) of isomer **3E**, which accounts for the low value of EC₅₀. ^b Pyrophosphonate **5Z** contains 1% (HPAEC relative area) of isomer **5E**, which accounts for the low value of EC₅₀.

**Figure 6.** $\gamma\delta$ -Fold increase at day 5 as compared to predose.

To better understand these observed differences in $\gamma\delta$ -T-cell stimulation by *Z*- and *E*-isomers, minimal energy conformations for both analogues (**3E** and **3Z**) were generated and superimposed. This simple modeling study reveals that only small geometrical shape variations between the *E*- and *Z*-isomers are observed. As shown in Figure 7, the distances between the terminal hydroxy group of the butenyl chain and the oxygen atom of the pyrophosphate moiety in the two isomers are 1.68 and 2.00 Å for the *Z*-isomer versus 1.76 and 2.02 Å for the *E*-isomer. Taking into account that the H-bond average length is around 2.7 Å, both isomers allow a similar intramolecular hydrogen bonding state. These data show that both strong conformational and energetic similarities exist between *E*- and *Z*-isomers, thus supporting the idea that any differences in

biological behavior depend on the respective geometric position of the methyl and methylenehydroxy groups. The observed enhanced stimulatory activity for the *E*-isomer is probably related to favored specific interactions within the cell antigen receptors, which occurred in biological media.

As expected, the presence of the diphosphate moiety is required for $\gamma\delta$ -T-cell optimal activity,^{8,17} while replacement of the pyrophosphate moiety by a pyrophosphonate group shows an equivalent stimulatory activity in both *Z*- and *E*-isomers (**5E** EC₅₀ = 0.91 versus **3E** EC₅₀ = 0.39 nM, and **5Z** EC₅₀ = 852 nM versus **3Z** EC₅₀ = 252 nM). Moreover, replacement of the diphosphate or diphosphonate moiety by a monophosphate or a monophosphonate drastically reduces $\gamma\delta$ -T-cell activation involving the β -phosphate bond hydrolysis to induce the activity. On the other hand, the methyl position change from 2 to 3 on the 1-hydroxy-butenyl chain indeed affects $\gamma\delta$ -T-cell activation, which is thought to involve a highly specific recognition.

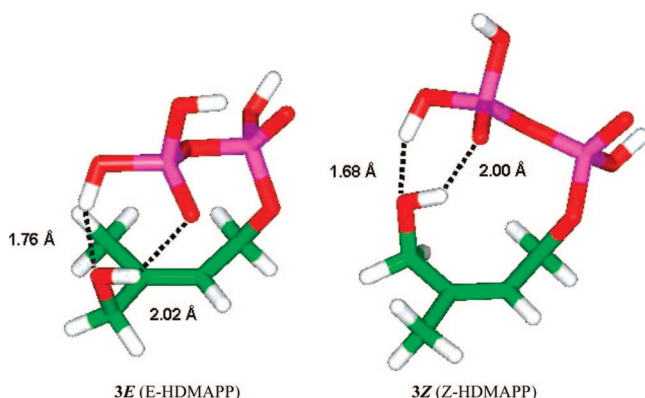
Conclusions

Overall, these results are of interest because we succeeded in synthesizing new pyrophosphonate analogues of BrHPP, a drug currently under clinical development,¹⁸ having potent $\gamma\delta$ -T-cell stimulation activity in vitro and that are far more stable than their parent pyrophosphate under acidic and stressed conditions. We have developed synthetic schemes that have led to both *Z*- and *E*-isomers of 1-hydroxy-(2 or 3)-methylbut-2-enyl pyrophosphonate. Confirmation of the structure has been obtained through an NMR study. Biological evaluation of the new analogues has shown that *E*-isomers are the most active derivatives, confirming for the pyrophosphate series, the ob-

Table 3. Comparative Stability Study between Pyrophosphonate and Pyrophosphate Analogues^a

	pyrophosphate 3E 0.3 mM solution		pyrophosphonate 5E 0.5 mM solution	
4 °C	≥7 days	stable over that period	5 °C	≥7 days
25 °C	7 days	5% degradation	25 °C	≥7 days
60 °C	24 h	14% degradation	50 °C	≥7 days
HCl 0.1 N at 60 °C	2 h	not detected	HCl 0.1 N at 40 °C ^a	2 h
H ₂ O ₂ 3% at 60 °C	2 h	4% degradation	H ₂ O ₂ 10% at 40 °C ^a	2 h
				stable over that period
				stable
				11% degradation
				0.5–1.0% degradation
				2% degradation

^a The % of degradation determination was carried out by ionic chromatography using a conductometric detection and estimated as % of relative area.

**Figure 7.** Molecular modeling representation of **3E** and **3Z**.

servations derived from the pyrophosphonate series. In vivo studies with the pyrophosphonate analogues led to the conclusion that the second generation $\gamma\delta$ -activators (*E*)-HDMAPP and (*E*)-C-HDMAPP are equally potent and around 20 times more potent than the first generation molecule BrHPP. Additionally, taking into account the results obtained in stability or excretion data, pyrophosphonate (*E*)-C-HDMAPP appears to present a better pharmacological profile than the pyrophosphate for clinical use. (*E*)-C-HDMAPP may, therefore, represent an attractive drug candidate for development in therapeutic indications, such as viral infections or cancer, where $\gamma\delta$ -T-cell stimulation is thought to be beneficial.

Experimental Section

Chemistry. General Methods. Starting materials and reagents were obtained from commercial suppliers and were used without purification and compounds **15**, **11**, **5E**, **7E**, and **4E** were provided by Carbogen Amcis AG (Schachenallee 29 CH-5001 Aarau, Switzerland). Tetrahydrofuran (THF) was distilled over sodium benzophenone ketyl immediately prior to use. Methylene dichloride (CH₂Cl₂) was distilled over P₂O₅ just prior to use. Nuclear magnetic resonance spectra were recorded at 300 MHz for ¹H, 75 MHz for ¹³C, and 121.5 MHz for ³¹P on a Bruker AVL-300 spectrometer and at 500 MHz for ¹H, 126 MHz for ¹³C on a Bruker Avance DRX-500 spectrometer. Elemental analyses were within $\pm 0.4\%$ of theoretical values for all compounds. Chemical shifts are expressed as δ units (part per million) downfield from TMS (tetramethylsilane). Mass spectral data was collected on a Bruker Esquire 2000 electrospray/ion trap instrument. Routine thin layer chromatographies (TLC) was performed on silica gel 60 F₂₅₄ aluminum plates (Merck) and flash chromatography was carried out with prepacked columns Merck SuperVarioFlash (silica gel, 15–40 Å). Ion exchange chromatography was performed with a strong cation exchange resin Dowex 50WX8 (H⁺ form; 100–200 mesh). High performance anion exchange chromatography (HPAEC) was performed on a Dionex DX600 System using a Dionex IonPac AS11 column (4 × 250 mm) and suppressed conductivity detection. Decompositions and melting temperatures (mp) were determined on a Mel-Temp II apparatus and are uncorrected.

(Z)-1-Chloro-3-methyl-4-(tetrahydropyran-2-yloxy)but-2-en (9a).¹² This intermediate was synthesized according to already published literature procedure. δ_{H} (300 MHz, CDCl₃) 1.51–1.80

(m, 6 H, CH₂CH₂CH₂), 1.84 (s, 3 H, CH₃CH=), 3.49–3.58 (m, 1 H, OCH), 3.83–3.91 (m, 1 H, OCH), 4.13–4.21 (m, 2 H, CH₂O), 4.16 (d, 2 H, *J* = 8.5 Hz, CH₂Cl), 4.59 (t, 1 H, *J* = 3.4 Hz, OCH), 5.62 (t, 1 H, *J* = 8.0 Hz, CH=C); δ_{C} (75 MHz; CDCl₃) 19.4, 21.8, 25.4, 30.5, 40.0, 62.2, 64.8, 97.5, 124.5, 138.3.

(Z)-1-Chloro-2-methyl-4-(tetrahydropyran-2-yloxy)but-2-en (9b).¹³ This intermediate was synthesized according to already published literature procedure. δ_{H} (300 MHz, CDCl₃) 1.48–1.87 (m, 6 H, CH₂CH₂CH₂), 1.90 (d, 3 H, *J* = 1.3 Hz, CH₃C=), 3.42–3.63 (m, 1 H, OCH), 3.82–3.94 (m, 1 H, OCH), 4.03–4.13 (m, 1 H, OCH), 4.11 (s, 2 H, CH₂Cl), 4.23–4.33 (m, 1 H, OCH), 4.63 (dd, 1 H, *J* = 2.8 Hz, *J* = 3.7 Hz, OCH), 5.56–5.63 (m, 1H, CH=C); δ_{C} (75 MHz; CDCl₃) 19.5, 21.7, 25.4, 30.6, 43.1, 62.3, 62.5, 97.9, 126.6, 136.0.

Methyl (3Z)-4-Methyl-5-(tetrahydropyran-2-yloxy)pent-3-enyl(morpholin-4-yl)phosphinate (12a). To a solution of methyl methyl(morpholin-4-yl)phosphinate **11** (450 mg, 2.2 mmol) in 10 mL of THF at -78 °C was added *n*-butyllithium (2.5 M solution in hexanes, 1.05 mL, 2.64 mmol). The mixture was maintained at -78 °C for 30 min. Then a solution of **9a** (1 g, 4.88 mmol) in 10 mL of THF was added dropwise. The mixture was allowed to warm to room temperature and stirred overnight. Then was added 5 mL of a saturated aqueous NH₄Cl, and the mixture was extracted with ether. The combined organic layers were washed with brine, dried over Na₂SO₄, filtered, and concentrated. The crude mixture was purified by silica gel (ethyl acetate/MeOH 95: 5) to give a colorless oil (260 mg, 34%); *R*_f 0.21 (ethyl acetate/MeOH 95: 5). δ_{H} (300 MHz, CDCl₃) 1.45–1.70 (m, 6 H, CH₂CH₂CH₂), 1.75 (s, 3 H, CH₃C=), 1.76–1.85 (m, 2 H, CH₂P), 2.26–2.38 (m, 2 H, CH₂CH₂P), 2.97–3.20 (m, 4 H), 3.44–3.50 (m, 1 H, OCH), 3.56 (s, 2H), 3.60 (m, 5H), 3.64–3.67 (m, 1 H), 3.79–3.86 (m, 1 H, OCH), 4.0–4.10 (m, 1 H), 4.53 (t, 1 H, *J* = 3.4 Hz, OCH), 5.32 (t, 1 H, *J* = 7.2, CH=C); δ_{C} (75 MHz; CDCl₃) 14.1, 19.4 (d, *J* = 3.8 Hz), 20.4 (d, *J* = 2.2 Hz), 25.4, 25.7 (d, *J* = 129.0 Hz), 30.5, 43.9, 50.0 (d, *J* = 7.1 Hz), 62.0 (d, *J* = 6.7 Hz), 65.1 (d, *J* = 2.6 Hz), 67.2 (d, *J* = 4.9 Hz), 97.4, 127.9 (d, *J* = 17.1 Hz), 133.1; δ_{P} (121.5 MHz, CDCl₃) 34.7.

Methyl (3Z)-3-Methyl-5-(tetrahydropyran-2-yloxy)pent-3-enyl(morpholin-4-yl)phosphinate (12b). To a solution of methyl methyl(morpholin-4-yl)phosphinate **11** (450 mg, 2.2 mmol) in 10 mL of THF at -78 °C was added *n*-butyllithium (2.5 M solution in hexanes, 1.05 mL, 2.64 mmol). The mixture was maintained at -78 °C for 30 min. Then was added dropwise a solution of **9b** (1 g, 4.88 mmol) in 10 mL of THF. The mixture was allowed to reach to room temperature and stirred overnight. Then was added 5 mL of a saturated aqueous NH₄Cl, and the mixture was extracted with ether. The combined organic layers were washed with brine, dried over Na₂SO₄, filtered, and concentrated. The crude mixture was purified by silica gel (ethyl acetate/MeOH 95: 5) to give a colorless oil (260 mg, 34%); *R*_f 0.21 (ethyl acetate/MeOH 95:5). δ_{H} (300 MHz, CDCl₃) 1.47–1.74 (m, 6 H, CH₂CH₂CH₂), 1.76 (d, 3 H, *J* = 1.1 Hz, CH₃C=), 1.79–1.92 (m, 2 H, CH₂P), 2.27–2.42 (m, 2 H, CH₂CH₂P), 3.05–3.24 (m, 4 H), 3.45–3.57 (m, 1 H, OCH), 3.61 (s, 2H), 3.66 (m, 5H), 3.82–3.94 (m, 1 H, OCH), 4.00 (dd, 1 H, *J* = 11.8 Hz, 7.5 Hz, OCH₂C=), 4.23 (dd, 1 H, *J* = 11.9 Hz, 6.4 Hz, OCH₂C=), 4.57–4.67 (m, 1 H, OCH) 5.41 (t, 1 H, *J* = 6.8 Hz, CH=C); δ_{C} (75 MHz; CDCl₃) 19.6 (d, *J* = 4.4 Hz), 23.0, 24.3 (d, *J* = 129.5 Hz), 24.6 (d, *J* = 3.8 Hz), 25.4, 30.7 (d, *J* = 1.7 Hz), 44.0, 50.2 (d, *J* = 7.1 Hz), 62.3 (d, *J* = 7.1 Hz), 63.1 (d, *J* = 3.3 Hz), 67.3, 67.4, 97.9, 122.5 (d, *J* = 4.4 Hz), 139.3 (d, *J* = 17.0 Hz); δ_{P} (121.5 MHz, CDCl₃) 34.7.

General Procedure for Pyrophosphorylation of 9a, 9b, 15, and Crystallization of Resulting Compounds. To a solution of 2.64 g of Tris(tetra-*n*-butylammonium) hydrogen pyrophosphate (2.93 mmol) in 10 mL of acetonitrile was slowly added at 0 °C a solution of the chloride compound (300 mg, 1.46 mmol) in THF (5 mL). The mixture was then allowed to stir and warm to room temperature overnight. The solution was concentrated by evaporation under reduced pressure. The resulting oil was dissolved in water (10 mL). The solution was passed through a column of Dowex 50WX8 (NH₄⁺ form), which had been equilibrated with 50 mL of a solution of 1% isopropanol/NH₄HCO₃ 25 mM. The column was eluted with 40 mL of 1% isopropanol/NH₄HCO₃ 25 mM. The collected fraction was lyophilized and a white solid was obtained. The residue was dissolved with 7 mL of solution of NH₄HCO₃ 25 mM and 22 mL of a mixture of isopropanol/CH₃CN 50/50 were added. The precipitate was removed, and the filtrate was concentrated.

Crystallization.¹⁹ A total of 1 equiv of ammonium salt compound (THP protected) is diluted with deionized water at room temperature. The aqueous solution obtained is loaded on a column containing 120 mequiv of Dowex 50WX8-200 cationic resin (H⁺ form), then eluted with 90 mL of deionized water (deprotection/acidification step). A 0.2 M methanolic solution of the benzathine base was then added slowly while stirring to the acidic solution until equivalent pH. The resulting mixture was a colorless solution. The entire amount of solvent was removed by evaporation under reduced pressure at 40 °C, and benzathine salt at the amorphous state (white solid) was obtained. This residue was homogenized with 30 mL of methanol while stirring at room temperature for 2 h. The resulting suspension was filtered and the isolated solid phase was mixed with 15 mL of ethanol at room temperature. The temperature was then progressively decreased down to 10 °C followed by a maturation step (10 temperature cycles between 45 and 10 °C with a 15°/h cooling rate). The last cycle was stopped at 10 °C (during the cooling phase), and the solid phase was collected by filtration through a glass filter and allowed to dry at ambient atmosphere until constant weight.

(2Z)-1-Hydroxy-2-methylbut-2-enyl-4-diphosphate Benzathine salt (3Z). Isolated as a white powder (258 mg, 35%). Mp: 165 °C (decomp). Isomeric ratio (*cis/trans*) 98/02. δ_{H} (500 MHz, D₂O) 1.80 (s, 3 H, CH₃C=), 3.45 (s, 4 H, NCH₂CH₂N), 4.12 (s, 2 H, CH₂OH), 4.29 (s, 4 H, 2 C₆H₅CH₂N), 4.46 (t, 2 H, J 6.3 Hz, CH₂OP), 5.57 (t, 1 H, J = 7.0 Hz, CH=C), 7.49 (m, 10 H, 2 C₆H₅); δ_{C} (126 MHz; D₂O) 20.7, 42.7, 51.7, 57.7, 60.1, 62.2 (d, J_{CP} = 5.1 Hz), 123.5 (d, J_{CP} 8.0 Hz), 129.6, 130.0, 130.1, 130.4, 140.0; δ_{P} (121.5 MHz, D₂O) -10.5 (br s). ESI-MS *m/z* 261 [M - H]⁻.

(2E)-1-Hydroxy-2-methylbut-2-enyl-4-diphosphate benzathine salt (3E). Isomeric ratio (*trans/cis*) 99/01. δ_{H} (300 MHz, D₂O) 1.67 (s, 3 H, CH₃C=), 3.45 (br s, 4 H, NCH₂CH₂N), 3.98 (s, 2 H, CH₂OH), 4.28 (s, 4 H, 2 C₆H₅CH₂N), 4.49 (t, 2 H, J = 6.8 Hz, CH₂OP), 5.60 (t, 1 H, J = 6.4 Hz, CH=C), 7.50 (m, 10 H, 2 C₆H₅); δ_{C} (75 MHz; D₂O) 13.4, 42.7, 51.7, 57.7, 62.8 (d, J_{CP} = 4.6 Hz), 66.7, 120.5 (d, J_{CP} = 7.5 Hz), 129.6, 130.0, 130.1, 130.4, 140.2; δ_{P} (121.5 MHz, D₂O) -10.3 (d, J 20.0 Hz), -10.7 (d, J = 20.0 Hz). ESI-MS *m/z* 261 [M - H]⁻.

(2Z)-1-Hydroxy-2-methylpent-2-enyl-pyrophosphonate Benzathine Salt (5Z). Isolated as a white powder (145 mg, 23%). Mp: 152 °C. Isomeric ratio (*cis/trans*) 99/01. δ_{H} (500 MHz, D₂O) 1.65–1.73 (m, 2 H, CH₂P), 1.75 (s, 3 H, CH₃C=), 2.25–2.35 (m, 2 H, CH₂CH), 3.44 (s, 4 H, NCH₂CH₂N), 4.11 (s, 2 H, CH₂OH), 4.28 (s, 4 H, 2 C₆H₅CH₂N), 5.42 (t, 1 H, J = 7.2 Hz, CH=C), 7.41–7.56 (m, 10 H, 2 C₆H₅); δ_{C} (126 MHz; D₂O) 20.8, 21.5 (d, J_{CP} = 3.8 Hz), 28.3 (d, J_{CP} = 137.0 Hz), 42.8, 51.7, 60.2, 128.8 (d, J_{CP} = 17.6 Hz), 129.6, 130.0, 130.1, 130.5, 134.20; δ_{P} (121.5 MHz, D₂O) -10.5 (d, J = 25 Hz), 19.1 (d, J = 26 Hz). ESI-MS *m/z* 259 [M - H]⁻.

(2E)-1-Hydroxy-2-methylpent-2-enyl-pyrophosphonate Benzathine Salt (5E). Isomeric ratio (*trans/cis*) 99/01. δ_{H} (300 MHz, D₂O) 1.66 (s, 3 H, CH₃C=), 1.70–1.77 (m, 2 H, CH₂P), 2.21–2.33 (m, 2 H, CH₂CH), 3.47 (s, 4 H, NCH₂CH₂N), 3.97 (s, 2 H, CH₂OH), 4.30 (s, 4 H, 2 C₆H₅CH₂N), 5.43 (t, 1 H, J = 6.9 Hz, CH=C), 7.51 (m, 10 H, 2 C₆H₅); δ_{C} (75 MHz; D₂O) 13.3, 21.5 (d, J_{CP} =

4.8 Hz), 27.9 (d, J_{CP} = 137.5 Hz), 42.9, 51.8, 67.8, 126.8 (d, J_{CP} = 17.4 Hz), 129.7, 130.1, 130.2, 130.5, 134.9; δ_{P} (121.5 MHz, D₂O) -10.5 (d, J = 25 Hz), 19.4 (d, J = 25 Hz). ESI-MS *m/z* 259 [M - H]⁻.

(2E)-1-Hydroxy-3-methylbut-2-enyl-diphosphate Sodium Salt (4E). δ_{H} (500 MHz, D₂O) 1.69 (3 H, s, CH₃C=), 4.15 (2 H, d, J = 7.0 Hz, CH₂OH), 4.33 (2 H, d, J = 7.2 Hz, CH₂OP), 5.68 (1 H, tq, J = 7.0 Hz, 1.0 Hz, HC=); δ_{C} (75 MHz, D₂O) 13.4, 58.3, 71.2 (d, J_{CP} = 5.8 Hz), 124.7, 136.6 (d, J_{CP} = 7.7 Hz); δ_{P} (121.5 MHz, D₂O) -9.5 (br s), -10.5 (br s). ESI-MS *m/z* 261 [M - H]⁻.

(2Z)-1-Hydroxy-3-methylbut-2-enyl-diphosphate Benzathine Salt (4Z). Isolated as a white powder (360 mg, 51%). Mp: 180 °C. Isomery *cis* 100%. δ_{H} (500 MHz, D₂O) 1.82 (s, 3 H, CH₃C=), 3.45 (br s, 4 H, NCH₂CH₂N), 4.15 (d, 2 H, J = 7.3 Hz, CH₂OH), 4.29 (s, 4 H, 2 C₆H₅CH₂N), 4.46 (d, 2 H, J = 6.4 Hz, CH₂OP), 5.59 (t, 1 H, J = 7.0 Hz), 7.49 (m, 10 H, 2 C₆H₅); δ_{C} (75 MHz; D₂O) 20.7, 42.8, 51.7, 64.5 (d, J = 5.4 Hz), 127.1, 129.6, 130.0, 130.1, 130.4, 136.0; δ_{P} (121.5 MHz, D₂O) -10.6 (br s). ESI-MS *m/z* 261 [M - H]⁻.

(2Z)-1-Hydroxy-3-methylpent-2-enyl-pyrophosphonate Benzathine Salt (6). Isolated as a white powder (126 mg, 44%). Mp 161–162 °C. Isomery *cis* 100%. δ_{H} (500 MHz, D₂O) 1.48–1.83 (m, 2 H, CH₂P), 1.72 (s, 3 H, CH₃C=), 2.18–2.40 (m, 2 H, CH₂CH₂P), 3.46 (s, 4 H, NCH₂CH₂N), 4.09 (d, 2 H, J = 7.3 Hz, CH₂OH) 4.29 (s, 4 H, 2 C₆H₅CH₂N), 5.39 (t, 1 H, J = 7.2 Hz, HC=), 7.49 (m, 10 H, 2 C₆H₅); δ_{C} (126 MHz, D₂O) 22.4, 25.3 (d, J_{CP} = 4.4 Hz), 26.9 (d, J_{CP} = 137 Hz), 42.7, 51.7, 57.7, 122.9 (d, J_{CP} = 17.6 Hz), 129.6, 130.0, 130.1, 130.4, 141.4 (d, J_{CP} = 16.7 Hz); δ_{P} (121.5 MHz, D₂O) -10.5 (d, J = 26 Hz), 19.1 (d, J = 26 Hz). ESI-MS, *m/z* 259 [M - H]⁻.

(2E)-1-Hydroxy-2-methylpent-2-enyl-phosphonate Benzathine Salt (7E). Isolated as a white powder. Isomeric ratio (*trans/cis*) 99/01. δ_{H} (300 MHz, D₂O) 1.49–1.63 (m, 2 H, CH₂P), 1.66 (s, 3 H, CH₃C=), 2.17–2.33 (m, 2 H, CH₂CH), 3.44 (s, 4 H, NCH₂CH₂N), 3.96 (s, 2 H, CH₂OH), 4.28 (s, 4 H, 2 C₆H₅CH₂N), 5.48 (t, 1 H, J = 6.8 Hz, CH=C), 7.50 (m, 10 H, 2 C₆H₅); δ_{C} (75 MHz; D₂O) 13.3, 21.9 (d, J_{CP} = 4.4 Hz), 28.1 (d, J_{CP} = 131.7 Hz), 43.0, 51.9, 67.9, 127.1 (d, J_{CP} = 17.0 Hz), 129.7, 130.1, 130.2, 130.5, 134.8; δ_{P} (121.5 MHz, D₂O) 25.8. ESI-MS, *m/z* 179 [M - H]⁻.

(2Z)-1-Hydroxy-2-methylpent-2-enyl-phosphonate Benzathine Salt (7Z). Isolated as a white powder (107 mg, 13%). Mp 114–115 °C. Isomeric ratio (*cis/trans*) 99/01. δ_{H} (500 MHz, D₂O) 1.51–1.64 (m, 2 H, CH₂P), 1.74 (s, 3 H, CH₃C=), 2.18–2.31 (m, 2 H, CH₂CH), 3.45 (s, 4 H, NCH₂CH₂N), 4.10 (s, 2 H, CH₂OH), 4.28 (s, 4 H, 2 C₆H₅CH₂N), 5.42 (t, 1 H, J = 7.5 Hz, CH=C), 7.40–7.57 (m, 10 H, 2 C₆H₅); δ_{C} (126 MHz; D₂O) 20.8, 21.7 (d, J_{CP} = 3.6 Hz), 28.5 (d, J_{CP} = 131.5 Hz), 42.7, 51.8, 60.2, 129.0 (d, J_{CP} = 16.7 Hz), 129.6, 130.0, 130.1, 130.4, 134.1; δ_{P} (121.5 MHz, D₂O) 26.4. ESI-MS *m/z* 179 [M - H]⁻.

(2Z)-1-Hydroxy-3-methylpent-2-enyl-phosphonate Benzathine Salt (8). Isolated as a white powder (59 mg, 20%). Mp 158 °C. Isomery *cis* 100%. δ_{H} (500 MHz, D₂O) 1.59–1.69 (m, 2 H, CH₂P), 1.75 (s, 3 H, CH₃C=), 2.22–2.33 (m, 2 H, CH₂CH), 3.45 (s, 4 H, NCH₂CH₂N), 4.10 (d, 2 H, J = 7.0 Hz, CH₂OH), 4.29 (s, 4 H, 2 C₆H₅CH₂N), 5.40 (t, 1 H, J = 6.9 Hz, CH=C), 7.42–7.55 (m, 10 H, 2 C₆H₅); δ_{C} (126 MHz; D₂O) 22.3, 25.7 (d, J_{CP} = 3.6 Hz), 27.1 (d, J_{CP} = 132.2 Hz), 42.7, 51.8, 57.7, 122.7 (d, J_{CP} = 16.7 Hz), 129.6, 130.0, 130.1, 130.4, 141.6; δ_{P} (121.5 MHz, D₂O) 26.3. ESI-MS *m/z* 179 [M - H]⁻.

Molecular Modeling. Molecular Mechanics. Calculations were performed on a SGI O2 platform running Macromodel version 6.5 (Schrödinger Inc.). Conformational minima were found using the modified MMFFs (1994 parameters) force field as implemented and completed in the Macromodel program.²⁰ Built structures were minimized to a final rms gradient ≤ 0.01 kJ·Å⁻¹·mol⁻¹ via the truncated newton conjugate gradient (TNCG) method (500 cycles). In all cases, the extended cutoff option was used throughout (VdW = 8 Å, electrostatic = 20 Å, and H-bond = 4 Å).

Monte Carlo-Style Conformational Search. This search is implemented in MacroModel.^{21,22} The automatic setup has been selected, that is, single bonds variable, chiral centers set, and flexible ring opened. To ensure convergence, 2000 steps were made per input structure, in an energy range of 10 kJ·mol⁻¹ (solution accessible conformation). Each conformer was fully minimized (5000 cycles, TNCG method, rms ≤ 0.01 kJ·Å⁻¹·mol⁻¹, MMFF94s force field). The least-used structures were used as starting geometries only if their energies were within the energetic window (10 kJ·mol⁻¹ of the lowest energy structure yet found). Calculations were considered convergent when each conformation has been found at least three times. Following the Monte Carlo search, a cluster analysis was performed with Xcluster 1.5,²³ using all heavy atoms rms as distance criterion selection. This approach leads to a set of clusters, each of them being a family of conformers. In Xcluster, a conformer is belonging to a cluster if it lies within the threshold distance of any component of this cluster and at more than this threshold distance of all components of all other clusters. For each molecule, a representative conformer of each cluster was saved and used for superimposition.

Biological Procedures. In Vitro TNF-α Release Bioassay. This standardized assay is based on the dosage of TNF-α released within hours by activated γδ-cells. Responder cells are generated from healthy donor PBMC cultured 10 to 14 days in the presence of BrHPP and renewed IL-2 (Proleukin(R), Chiron). After this culture, γδ-cells account for more than 90% of total cells and they are stored frozen before use. On the day of the test, 180000 thawed cells are put in 200 μL culture medium in the presence of increasing concentrations of substances to be tested. Systematically, as a positive control, dose-ranging concentrations of BrHPP are used (5 μM to 0.064 nM). After overnight stimulation, supernatants are harvested and dosed for TNF-α concentration with a commercial EIA test (Immunotech-Beckman-Coulter), according to the manufacturer's instructions. A series of tests is accepted when simultaneous control BrHPP EC₅₀ is found at 25 ± 3 nM.

Animals. All studies were subjected to approval by local ethical committees. Husbandry conditions conformed to the European requirements, comprising monitored temperature, humidity, air change and lighting cycle. Animals were housed individually in stainless steel cages. Food was composed of expanded complete primate diet (U.A.R., Villemoisson, Epinay/Orge, France or Special Diet Services: OWM (E) short SQC) analyzed for the absence of chemical and bacterial contaminants and supplemented daily with fresh fruits and/or vegetables.

When required, animals were anaesthetized with intramuscular injection of 6 mg/kg Zoletil 100 (Tiletamine-Zolazepam, Virbac, Carros, France) before any infusion.

- **Experiment with 3E.** A total of eight purpose bred male cynomolgus monkeys (*M. fascicularis*) were supplied by Noveprim (Ferney S.E., Mahebourg, Mauritius). At the beginning of the study, body weights ranged from 3.5 to 4 kg and ages from 37 to 41 months.

(E)-HDMAPP (batch INPA10-01) was administered i.v. by 30 min infusions in a total volume of 50 mL with Ringer lactate as vehicle. Injected doses: 2.5, 0.5, 0.1, and 0.02 mg/kg.

- **Experiment with 5E.** A total of 14 purpose bred cynomolgus monkeys (7 males and 7 females) were supplied by Noveprim. At the beginning of the study, body weights ranged from 1.8 to 3.5 kg and ages from 24 to 36 months.

(E)-C-HDMAPP (batch NE-018920-A-2-4 AP 1#1) was administered i.v. as bolus injections of 0.6 to 3 mL Ringer lactate, according to dose and body weight. Injected doses: 10, 5, 2.5, 0.5, 0.1, and 0.02 mg/kg.

All animals were cotreated with IL-2 (Proleukin(R), Chiron) to sustain γδ-cell proliferation, daily for five consecutive days, with s.c. injections of 0.6 M IU in 300 μL water. Blood was drawn predose and at days 4, 5, 7, 11, and 14 after each administration for flow cytometry analysis of blood cellular populations of interest. Blood samples (1 to 4 mL) were withdrawn from femoral vessels/artery into heparin-lithium containing tubes. Tubes were shipped overnight at room temperature (RT) before flow cytometry analyses.

Flow Cytometry. Peripheral γδ-lymphocytes were analyzed by flow cytometry on total monkey blood, after triple staining with anti-Vγ9-FITC, anti-CD3PE, and anti-CD69PC5 antibodies (Vγ9-FITC: 7B6 clone, produced, purified and FITC-coupled at Innate Pharma; CD3-PE: SP34 clone, BD Biosciences Pharmingen, Le Pont de Claix, France; CD69PC5: FN50 clone, Immunotech-Beckman-Coulter, Marseilles, France). Briefly, 50 μL of monkey blood was incubated 15 min at RT with 10 μL anti-Vγ9-FITC, 5 μL of anti-CD3-PE, and 5 μL of anti-CD69PC5 antibodies. Antibodies were washed with 3 mL 1X PBS, centrifuged for 4 min at 1300 rpm at RT, and the supernatant was discarded. Red cells were lysed with the OptiLyse C reagent (Immunotech-Beckman-Coulter) according to the manufacturer's instructions. At the final step, stained white blood cells were recovered by centrifugation and resuspended in 300 μL of 1X PBS + 0.2% PFA. Immediately before analysis, 50 μL calibrated flow count fluorospheres (Immunotech-Beckman-Coulter) were added to the cells for absolute number counting of the populations of interest. Flow cytometry was performed on a FC500 apparatus (Beckman-Coulter, Roissy, France).

Acknowledgment. We thank Dr. Emad El Sayed (Carbogen Amcis), Monique Moyne (Biomatech), Françoise Horand (MDS Pharma Services), Keith Dudley for the critical reading of the manuscript, and we gratefully acknowledge the help and discussion of Prof. Michel Maffei (Université Paul Cézanne).

Supporting Information Available: Elemental analysis data. This material is available free of charge via the Internet at <http://pubs.acs.org>.

References

- (1) Constant, P.; Davodeau, F.; Peyrat, M. A.; Poquet, Y.; Puzo, G.; Bonneville, M.; Fournie, J. J. Stimulation of human gamma delta T cells by nonpeptidic mycobacterial ligands. *Science* **1994**, *264*, 267–270.
- (2) Allison, T. J.; Winter, C. C.; Fournie, J. J.; Bonneville, M.; Garboczi, D. N. Structure of a human gamma delta T-cell antigen receptor. *Nature* **2001**, *411*, 820–824.
- (3) Bonneville, M.; Scotet, E. Human Vγ9Vδ2 T cells: Promising new leads for immunotherapy of infections and tumors. *Curr. Opin. Immunol.* **2006**, *18*, 1–8.
- (4) Sicard, H.; Fournie, J. J. Metabolic routes as targets for immunological discrimination of host and parasite. *Infect. Immun.* **2000**, *68*, 4375–4377.
- (5) Espinosa, E.; Belmant, C.; Pont, F.; Luciani, B.; Poupot, R.; Romagné, F.; Brailly, H.; Bonneville, M.; Fournie, J. J. Chemical synthesis and biological activity of bromohydrin pyrophosphate, a potent stimulator of human γδ T cells. *J. Biol. Chem.* **2001**, *276*, 18337–18344.
- (6) Amslinger, S.; Kis, K.; Hecht, S.; Adam, P.; Rohdich, F.; Arigoni, D.; Bacher, A.; Eisenreich, W. Biosynthesis of terpenes. Preparation of (E)-1-hydroxy-2-methylbut-2-enyl 4-diphosphate, an intermediate of the deoxyxylulose phosphate pathway. *J. Org. Chem.* **2002**, *67*, 4590–4594.
- (7) Hecht, S.; Amslinger, S.; Jauch, J.; Kis, K.; Trentinaglia, V.; Adam, P.; Eisenreich, W.; Bacher, A.; Rohdich, F. Studies on the non-mevalonate isoprenoid biosynthetic pathway. Simple methods for preparation of isotope-labeled (E)-1-hydroxy-2-methylbut-2-enyl 4-diphosphate. *Tetrahedron Lett.* **2002**, *43*, 8929–8933.
- (8) Amslinger, S.; Hecht, S.; Rohdich, F.; Eisenreich, W.; Adam, P.; Bacher, A.; Bauer, S. Stimulation of Vγ9/Vδ2 T-lymphocyte proliferation by the isoprenoid precursor, (E)-1-hydroxy-2-methylbut-2-enyl 4-diphosphate. *Immunobiology* **2007**, *212*, 47–55.
- (9) Patani, G. A.; LaVoie, E. J. Bioisosterism: A rational approach in drug design. *Chem. Rev.* **1996**, *96*, 3147–3176.
- (10) Thornber, C. W. Isosterism and molecular modification in drug design. *Chem. Soc. Rev.* **1979**, *8*, 563–580.
- (11) Sicard, H.; Ingoure, S.; Luciani, B.; Serraz, C.; Fournie, J. J.; Bonneville, M.; Tiollier, J.; Romagne, F. In vivo immunomanipulation of V gamma 9V delta 2 T cells with a synthetic phosphoantigen in a preclinical nonhuman primate model. *J. Immunol.* **2005**, *175*, 5471–5480.
- (12) Cooper, J.; Knight, D. W.; Gallagher, P. T. Total synthesis of (–)-α-kainic acid. *J. Chem. Soc., Perkin Trans. 1* **1992**, *5*, 553–559.
- (13) Kondo, K.; Matsui, K.; Negishi, A. Polypropenyl sulfides. *Jpn. Kokai Tokyo Koho*, JP 49042627, 1974.

- (14) Valentijn, A. R. P. M.; van der Marel, G. A.; Cohen, L. H.; van Boom, J. H. An expeditious synthesis of pyrophosphate analogues of farnesyl pyrophosphate using the phosphorylating agent methyl methylphosphonomorpholidate. *Synlett* **1991**, 9, 663–664.
- (15) Pont, F.; Luciani, B.; Belmant, C.; Fournie, J. J. Characterization of phosphoantigens by high-performance anion-exchange chromatography-electrospray ionization ion trap mass spectrometry and nanoelectrospray ionization ion trap mass spectrometry. *Anal. Chem.* **2001**, 73, 35623569.
- (16) Poquet, Y.; Constant, P.; Peyrat, M. A.; Poupot, R.; Halary, F.; Bonneville, M.; Fournie, J. J. High-pH anion-exchange chromatographic analysis of phosphorylated compounds: Application to isolation and characterization of nonpeptide mycobacterial antigens. *Anal. Biochem.* **1996**, 243, 119–126.
- (17) Belmant, C.; Espinosa, E.; Halary, F.; Tang, Y.; Peyrat, M. A.; Sicard, H.; Kozikowski, A.; Buelow, R.; Poupot, R.; Bonneville, M.; Fournie, J. J. A chemical basis for selective recognition of nonpeptide antigens by human delta T cells. *FASEB J.* **2000**, 14, 16691670.
- (18) Bennouna, J.; Medioni, J.; Rolland, F.; Misset, J. L.; Campone, M.; Sicard, H.; Tiollier, J.; Romagné, F.; Douillard, J. Y.; Calvo, F. Phase I clinical trial of bromohydrine pyrophosphate, BrHPP (phosphostim), a V α 9V δ 2 T lymphocytes agonist in combination with low dose interleukin-2 in patients with solid tumors. *J. Clin. Oncol.* **2005**, 23, 174.
- (19) Coquerel, G.; Aubin, E. Preparation of phosphoantigens salts of organic bases and methods for their crystallization. *PCT Int. Appl. WO* 2007039635, 2007.
- (20) Halgren, T. A. Merck molecular force field. I. Basis form, scope parameterization, and performance of MMFF94. *J. Comput. Chem.* **1996**, 17, 490–519.
- (21) Chang, G.; Guida, W. C.; Still, W. C. An internal-coordinate Monte Carlo method for searching conformational space. *J. Am. Chem. Soc.* **1989**, 111, 4379–4386.
- (22) Saunders, M.; Houk, K. N.; Wu, Y. D.; Still, W. C.; Lipton, M.; Chang, G.; Guida, W. C. Conformations of cycloheptadecane. A comparison of methods for conformational searching. *J. Am. Chem. Soc.* **1990**, 112, 1419–1427.
- (23) Shenkin, P. S.; McDonald, D. Q. Cluster analysis of molecular conformations. *J. Comput. Chem.* **1994**, 15, 899–916.

JM701101G